University of Tehran Press

Online ISSN: 2345-475X

DESERT

Home page: https://jdesert.ut.ac.ir/

Investigating the Impact of Climate Change on the Effective Indicators in Desertification and Predicting its Spatial Changes

Azam Sadat Hosseini Khezr Abad[1], Abbasali Vali[1*], Amirhossein Halabian[2], Mohammad Hossein Mokhtari[3], Seyyed Ali Mousavi[1]

[1] Drylands management department, Faculty of Natural Resources and Earth Sciences, University of Kashan, Kashan. Iran. E-mail: vali@kashanu.ac.ir
[2] Department of Geography, Payam Noor University, Tehran, Iran.
[3] Department of Desert and Arid Land Management, Faculty of Natural Resources and Desertology, Yazd University, Iran.

Article Info.

Article type:
Research Article

Article history:
Received: 06 Aug. 2024
Received in revised from: 13 Nov. 2024
Accepted: 09 Dec. 2024
Published online: 27 Dec. 2024

Keywords:
Desertification,
Downscaling,
Global Climate Models,
LARS-WG,
Forecasting,
Desert ecosystem.

ABSTRACT

Excessive dryness of arid regions has increased the intensity and spread of desertification. Investigating spatial and temporal patterns of desertification caused by climate change in the northwest of Yazd province using the Iranian model of desertification potential assessment (IMDPA) is one of the main objectives of this research. In this study, a twenty-year statistical period (2001-2020) was also selected as the base period to reveal climate change. And the precipitation and average temperature data collected from selected stations were downscaled with the BCC-CSM1-1 model from the CMIP5 series, under three radiative forcing scenarios RCP2.6, RCP4.5, and RCP8.5 using the LARS-WG6 simulator for the near future (period 2026-2055) and the far future (2071-2100). And the results of predicting climatic elements on the increase in the area of areas prone to desertification in the studied region were evaluated. The results showed that the rainfall in the final decades of this century is lower than in the period 2026-2055 and in some places is increasing or decreasing compared to the average of the base period. Temperatures will increase relative to baseline for both future periods. Also, based on the IMDPA model, 80.54 percent of the area of the region is in the severe desertification class in the base period. The intensity of climate-driven desertification in the distant future is more severe than in the near future and the base period. The largest changes in desertification classes in the near future are related to RCP2.6 and RCP4.5, and in the distant future are related to all scenarios. So that during this period, we will witness the transition and change of moderate and severe risk classes to severe and very severe classes, especially in RCP4.5. Therefore, at the end of this century, the intensity of desertification in the region will be more severe than in the base period and the near future.

Cite this article: Hosseini Khezr Abad, A.S., Vali, A., Halabian, A., Mokhtari, M.H., Mousavi, S.A. (2024). Investigating the impact of climate change on the effective indicators in desertification and predicting its spatial changes. DESERT, 29 (2), DOI: 10.22059/jdesert.2024.100148

DOI: 10.22059/jdesert.2024.100148

Publisher: University of Tehran Press

1. Introduction

Global warming, changes in precipitation and changes in the frequency of weather events increase the probability of climate change and change the annual and seasonal water supply (Refsgaard *et al*., 2013). Hydrological processes are highly sensitive to rainfall and temperature (Sharafati *et al*., 2020). Therefore, climate change causes changes in ecological and hydrological patterns, reducing the diversity and volume of vegetation, destroying forests, pastures and other managed lands, and finally, it causes drought and the spread of desertification (Purkey *et al*., 2008; Perez Marin *et al*., 2022). Due to the lack of basic understanding of the spatial and temporal variation of climatic elements, also due to the economic, social consequences and financial damages related to atmospheric events, climate change has become a major challenge in many countries (Shrestha *et al*., 2017). From this aspect, the introduction and recognition of climate change anomalies is very important, and effective planning requires the examination of current and predicted climate change scenarios.

The United Nations Convention to Combat Desertification (UNCCD[1], 1994) limits desertification to dry areas located between 30 degrees north and 30 degrees south latitudes. Arid and semi-arid regions with different degrees of drought, which have an area of approximately 66.7 million square kilometers, and nearly two billion people of the world's population live in these regions (Pinheiro Junior *et al*., 2019). So that their livelihood depends on the natural resources in the environment and 22% of the world's food is produced in these environments (Perez Marin *et al*., 2012). As a result of the current scenarios of climate change, it is predicted that the size of these areas will increase (Leon Sobrino, 2019). Among the most important effects of desertification, we can mention the reduction of food security and human health, drought and physical instability caused by severe and extensive dust storms, ecosystem destruction, threats to vital systems and settlements (Alori *et al*., 2020). These effects indicate the extraordinary impact of desertification and climate change processes on each other (Perez Marin *et al*., 2020). Therefore, recognizing and evaluating the rate of desertification in developing countries and its relationship with climate change is important and inevitable in planning strategies to reduce damage caused by this phenomenon.

Investigating the consequences of climate change in the phenomenon of desertification in different regions of the world is done using the common methods of combining criteria and indicators, which mostly relies on meteorological data such as rainfall and temperature, which is one of the most important. In Iran, we can refer to the IMDPA (Iranian Model of Desertification Potential Assessment) model and rainfall and drought persistence indicators.

Despite the importance of desertification and its relationship with climate change, few studies have been conducted in different regions of the world, we mention some of them: Mahmood and Babel (2013) in a research with straw-scale average rainfall data, at least and maximum temperature using the SDSM model with two scenarios A2 and B2 for three periods in the 2020s, 2050s and 2080s in Pakistan, they concluded that the intensity and frequency of rainfall and temperature will increase in the future. The maximum and minimum temperature in scenario A2 is 0.3-91.15 and 0.93-2.63 degrees Celsius respectively, and in scenario B2 it is 0.69-1.92 and 0.53-1.63 (℃) increases. Gulacha and Mulungu (2017) by evaluating rainfall and temperature using the HadCM3 simulation under two emission scenarios A2 and B2 and the SDSM statistical straw scale in the catchment area of Tanzania, reached the conclusion that in the period of 2020-2080, the maximum temperature with a rhythm The increase is 0.2-7.5 (℃) and the minimum temperature is accompanied by a decrease from -0.4 to -1.5 (℃). In research,

[1] United Nations Convention to Combat Desertification

(Almazroui *et al*., 2017) evaluated the uncertainty of temperature and rainfall changes simulated by the models of the fifth assessment report (AR5) under two scenarios 4.5 and 8.5 in Saudi Arabia and reached these results that the temperature is increasing in all parts of Saudi Arabia, while the rainfall will increase in some places and decrease in others. (Abbasian *et al.,* 2018) evaluated the performance of 37 general circulation models in the simulation of temperature and rainfall in Iran during the period of 1901-2005. The obtained results stated that most GCMs perform well in simulating annual and seasonal temperature in Iran, but most GCMs have poor skill in simulating rainfall, especially on a seasonal scale. However, for simulating temperature and rainfall in Iran, CMCC-CMS and MRI-CGCM3 models have been introduced as the best GCM, respectively. (Lee *et al*., 2019) used Medalos model and ESAs method in evaluating the sensitivity of land cover to desertification in Mongolia and reached these findings that desertification in the region is increasing strongly from 2003 to 2008. and the biggest role in the desertification of the region is related to climate and vegetation criteria. (Zhang *et al*., 2020) investigated and identified the impact of climate change on desertification in North China through the analysis of potential evapotranspiration and rainfall in research and concluded that during different periods of time, the desert Desertification has been developed and expanded a lot in China, and climate change is thought to be the main driving force behind the return of desertification in this country. (Javaherian *et al*., 2021) evaluated and forecasted the climatic parameters of the Lar Dam basin with the CanESM2 model and radiative forcing scenarios of 2.6, 4.5 and 8.5 for the years 2020-2060. The output of the findings showed that the average temperature will increase between 1.01 to 1.12 (℃) and the amount of rainfall will increase by 21.23% in the coming period. In a research, (Abuzaid and Abdelatif, 2022) evaluated desertification using the modified Madalus model and ESAs method by analyzing five indicators of climate, soil, vegetation, management and erosion in the northern Nile Delta region in Egypt. Based on the obtained results, 72% of the region was identified as sensitive to desertification, of which 70% is very critical and 2% is semi-critical.

In Iran, desertification is a serious threat because in 2015, from the climatic point of view, 55% of the country's lands are desert areas, and in these societies, desertification is a primary limitation for sustainable development (Sadeghiravesh *et al*., 2021). However, since climate is one of the most important factors affecting desertification, also considering the different rhythms of climate change in different parts of the world, long-term forecasting of climatic parameters of temperature and rainfall and its relationship with desertification It is an unavoidable necessity and has significant importance in natural resources studies (Tanarhte *et al.*, 2012). For this purpose, the current research was conducted with the aim of investigating the effect of climate change on the effective indicators in desertification. The existence of such research in the northwest of Yazd in order to investigate the desertification situation caused by climate change in the near and far future, in addition to determining the contribution of each of the climatic elements in the aggravation of this situation, it can provide suitable opportunities for control. To create the destructive practices of the earth by increasing the vegetation cover and soil protection and in the future to respond to the needs of the agricultural sector, which is directly and indirectly dependent on the provision of human food. Also, it is very important in planning to prevent the expansion of the desert and to prevent possible consequences in the future.

2. Materials and Methods

2.1. Study area

The research area in this research is Ashkezar city, 20 kilometers northwest of Yazd province. The area of the research area is about 1905.81 square kilometers (Figure 1). The geographical coordinates of the area include the eastern longitude of 53 degrees, 41 minutes and 31 seconds to 54 degrees, 26 minutes and 41 seconds and the northern latitude of 31 degrees, 45 minutes and 35 seconds to 32 degrees, 12 minutes and 59 seconds. The studied area is divided into three climatic classes based on the Selianinov system. AA: Absolutely Arid, A: Arid and SSA: Slight Semi-Arid (Figure 2).

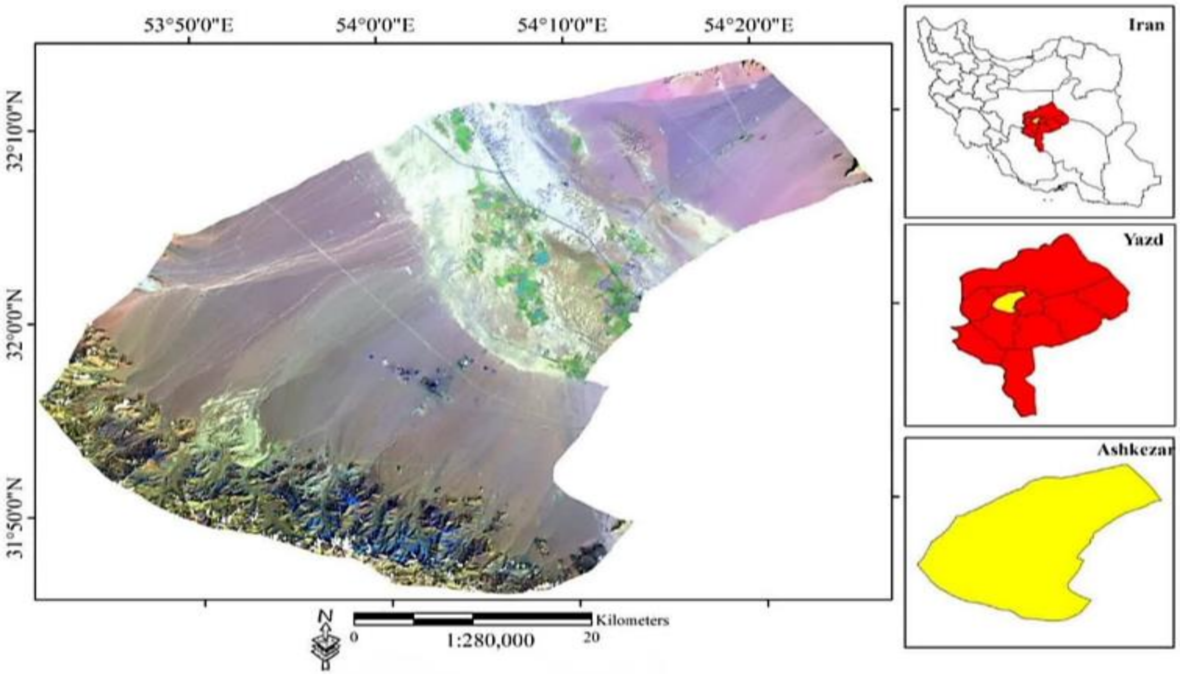

Fig 1. Location of the study area in a) Iran, b) Yazd province and, c) Landsat image

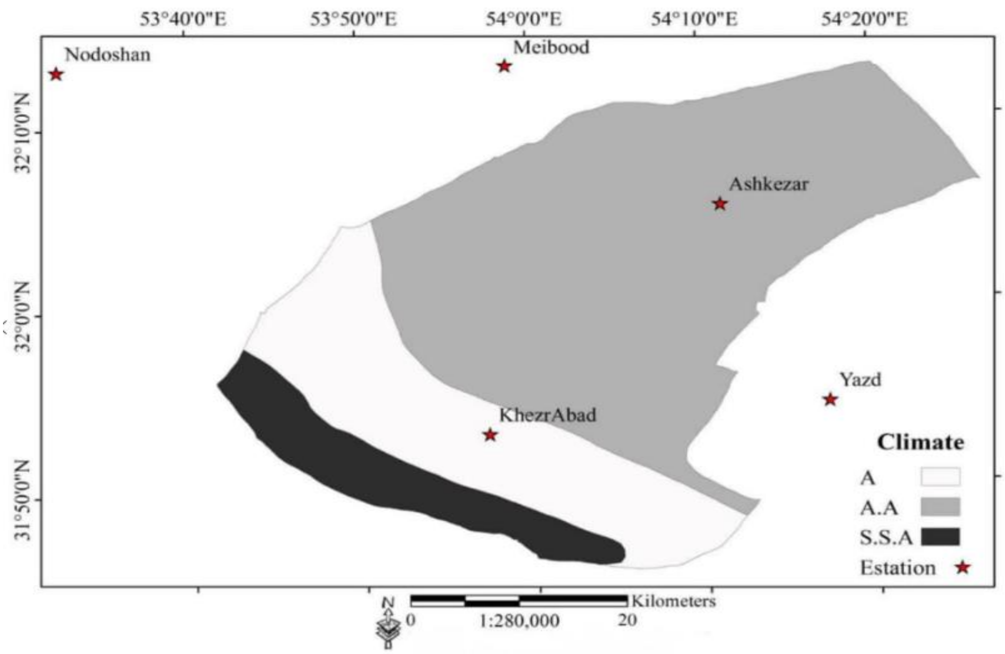

Fig 2. Climate classification map of the study area based on Selianinov method

2.2. Meteorology data

In this research, in order to prepare the data of meteorological stations, in addition to Ashkezar and Khezrabad stations, which were located inside the research area, the statistics of three other stations that were closer to the area in terms of geographical location have been used. Therefore, in order to investigate climatic elements, the daily parameters of rainfall, minimum and maximum temperature of five meteorological stations with a statistical period of twenty years (2001-2020) have been used (Table 1). Figure 2 shows the location of the studied stations in the region.

Table 1. Characteristics of the meteorological station the study

No.	Station Type	Name	Height (m)	Latitude E (DMS)	Longitude N (DMS)	Average Temprature(℃)	Annual Rain(mm)
1	synoptic	Yazd	1237	31° 54' 27"	54° 17' 39"	20.72	47.58
2	Climatology	Ashkezar	1140	32° 05' 38"	54° 11' 33"	19.66	48.82
3	Climatology	KhezrAbad	1733	31° 53' 03"	53° 57' 53"	18.57	93.82
4	synoptic	Meibood	1116	32° 13' 10"	53° 58' 52"	19.66	52.31
5	Climatology	Nodoshan	1994	32° 13' 27"	53° 32' 50"	14.85	81.37

2.3. Downscaling

In this research, in order to simulate and downscaling the data of the BCC-CSM1-1 model from the CMIP5 series, which has 2.6, 4.5, and 8.5 radiative forcing scenarios with a resolution of 12.77° × 2.81°, from the LARS-model WG6, which is one of the most famous models in forecasting climate data under current and future conditions, has been used. This model was developed by (Semenov and Barrow, 1977). Data generation by LARS-WG6 model is done in three stages, which include data calibration, data evaluation and micro scaling, and forecasted data generation for the future period. Based on this, for the implementation of this model in the current research, first the twenty-year statistical period (2001-2020) was considered as the basic and common statistical period, then the daily data required by the model including rainfall parameters, minimum and maximum temperature of 5 stations The meteorology mentioned in Table 1 was prepared from the General Directorate of Meteorology in Yazd during the basic period. After processing and sorting the data and preparing the input files, the model was executed for the base period and thus the calibration stage was performed. In the next step, to evaluate the data, several error statistics were used, including the coefficient of explanation (R^2), the normalized root mean squared error (NRMSE=Normalized Root Mean Squared Error) and the mean absolute error (MAE=Mean Absolute Error). Then the data generated by the model are evaluated with real data in the base period.

$$R^2 = \frac{\sum_{i=1}^{n}(O_i-\bar{O}_i)(E_i-\bar{E}_i)}{\sum_{i=1}^{n}(O_i-\bar{O}_i)^2(E_i-\bar{E}_i)^2} \quad (1)$$

$$NRMSE = \sqrt{\frac{\sum_{i=1}^{n}(O_i-E_i)^2}{n}} / O_i - E_i \quad (2)$$

$$NRMSE = \sqrt{\frac{\sum_{i=1}^{n}(O_i-E_i)^2}{n}} / O_i - E_i \quad (3)$$

That in these relationships; O_i: base period values (2001-2020); E_i: simulated period values; n: the total number of samples to be evaluated. The coefficient of explanation shows the correlation between the simulated values of the model and the base values.

After checking the results of the evaluation stage and ensuring the ability of the LARS-WG6 model in simulating meteorological data, this model is used to simulate the data of the BCC-CSM1-1 model from the CMIP5 series and to produce synthetic data for two time periods called 2055- 2026 (near future) and 2100-2071 period (far future), became using three radiative forcing scenarios namely RCP2.6, RCP4.5 and RCP8.5 (optimistic, moderate and pessimistic, respectively) approved by IPCC. The specifications of the radiative forcing scenarios are presented in Table 2.

Table 2. Specifications of Representative Concentration Pathways (RCP) used in the AR5 (IPCC, 2014)

Name	Radiative Forcing	CO_2 equiv (p.p.m.)	Temp anomaly (°C)	Pathway	SRES temp anomaly equiv
RCP8.5	In 21008.5wm^2	1370	4.9	Rising	SRES A1F1
RCP4.5	post 2100 4.5wm^2	650	2.4	Stabilization without overshoot	SRES B1
RCP2.6	3wm^2before2100, declining to2.6wm^2 by2100	490	1.5	Peak and decline	None

2.4. Assessment of desertification

In this research, the IMDPA model, which is one of the most common methods in Iran, was used to evaluate and prepare a map of desertification. The basis of work in this model is the map of work units (homogeneous units), which also has a special position in natural resources studies (Arami and Ownagh, 2017). In preparing the work unit map, the combination of basic maps such as slope maps, land use maps, geomorphological maps of the region and Google Earth images have been used. In this research, the scoring of each index was done inside separate work units.

The IMDPA model consists of 9 criteria: climate, soil, vegetation, wind erosion, geomorphology, water and irrigation, agriculture, urban and industrial development, and socio-economic (Ahmadi, 2006), which according to the topic of the research, the only climate criterion for the study of the desertification situation was used. The climate criterion is a natural criterion in the evaluation of the potential of desertification, and it directly creates effective indicators in the evaluation, and indirectly it is also part of the indicators of other criteria (Sepehr *et al.*, 2007; Sadeghiravesh *et al.*, 2021). Three indicators of annual rainfall, drought index and drought continuity were considered as key indicators of this criterion in desertification. Twenty-year rainfall statistics (2001-2020) of 5 meteorological stations were used to calculate the rainfall index.To investigate the drought index in this research, the drought index introduced by the University of Tehran (UTI) and the Bagnold-Gossen index or BGI (Relation 4 and 5) were used, and the decimal index was used to calculate the drought persistence index. This index is obtained based on the division of the probability distribution of the long-term rainfall statistics recorded at each station by tenths of the normal distribution, where each part is called a tenth.

$$\mathrm{BGI} = \sum_{i=1}^{n}(2\mathrm{T_i} - \mathrm{P_i}) \times \mathrm{K_i} \tag{4}$$

where in; T_i: average temperature in month i, P_i: total rainfall in month i, K_i = 0: if ($2T_i$-P_i) ≤0 in month i, and K_i= 1: if ($2T_i$-P_i)>0 in month i, (Pellegrini *et al.*, 2018).

$$UTI = -1.90 \times 10^{-3}(BGI)^2 + 1.23(BGI) - 124 \tag{5}$$

According to the conditions of the region, each index is weighted based on its impact on desertification (Table 3). Finally, the climate benchmark map was obtained from the geometric mean of the mentioned indicators according to equation 6 (Akbari *et al*., 2016).

$$Ceriteria - x = [(Index - 1).(Index - 2) \dots (Index - n]^{1/n} \quad (6)$$

Where in; Criteria-x is the climate criterion, Index: indicators and n: the number of indicators. An overview of the research process is schematically shown in Figure 3.

Table3. Scoring scheme for each index in the IMDPA model based on climate criteria (Arami, 2012)

No.	Climate Ceriteria			Desertification Class	
	Rain Index	UTI Drought Index	Persistence of Drought Index	Qualitative Class	Range of Class
1	280<	150-180	3-4 year	Low	0-1.5
2	150-280	120-150	5-6 year	moderate	1.51-2.5
3	75-150	90-120	6-7 year	sever	2.51-3.5
4	<75	<90	7year <	Very sever	3.51-4

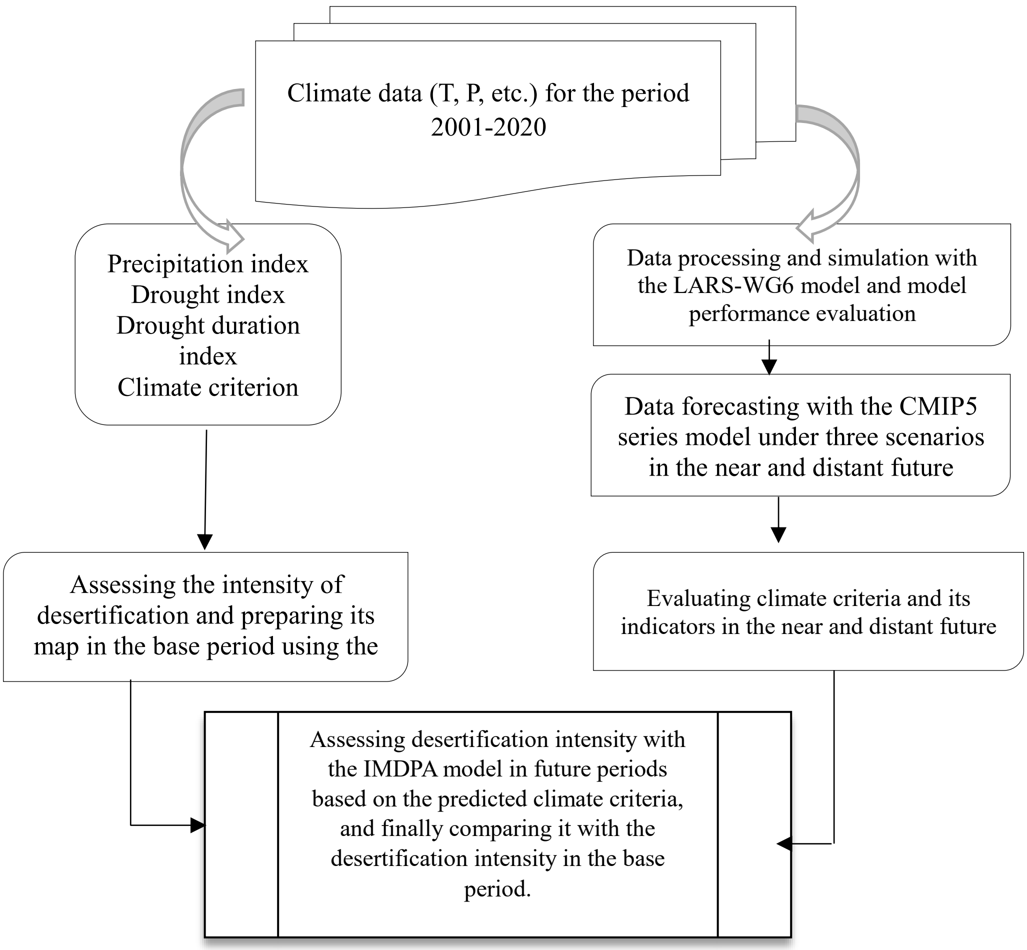

Fig. 3. Flowchart of research steps

2.5. Investigating the impact of climate change on the effective indicators in desertification

The forecasted climate data for all three radiative forcing scenarios RCP2.6, RCP4.5 and RCP8.5 in the near and far future periods are re-entered into the IMDPA desertification model and finally by comparing it with the base period, we estimate the impact of climate change in each scenario on the increase in desertification areas in the research area.

3. Results

3.1. Map of work units

According to the geomorphological features of the research area, the number of 12 work units has been separated in the area. 4 work units are located in the mountains and 8 work units are located in Pediment. Due to the lack of definition of evaluated parameters in residential and rock mass areas, these two separate facies are not evaluated and investigated as the working unit of the research area in desertification. Table 4 shows the names of work units and the area of each of them in the research area. Figure 4 shows the location of work units in the region. Upper plateaus and terraces with an area of more than 600 square kilometers cover most of the studied area.

Table4. Geomorphological units, types and facies in the research area

Union	Type	Facies geomorphological		Area (km^2)
Mountain	Mountain	Rock Mass	Rock Mass	69.44
	Hill	Birinzade of Rock	Birinzade of Rock	284.27
		Hill	Hill	11.06
		Water Erosion	Water Erosion in Mountain	111.95
Glacis (Pediment)	Denudation	Domain Plain	Domain Plain	47.04
		Plateau and Terrace	Upper Plateaus and terraces	600.23
	Epandage	Deposite	Rock-Shaped fan Deposites	485.08
		Mixed Land	Mixed Land	178.96
		Lowland	Lowland	14.92
	Dennoyoges	Sand Dune	Sand Dune	43.95
		Agricultur	Agricultur	18.60
		Urban	Urban	40.31

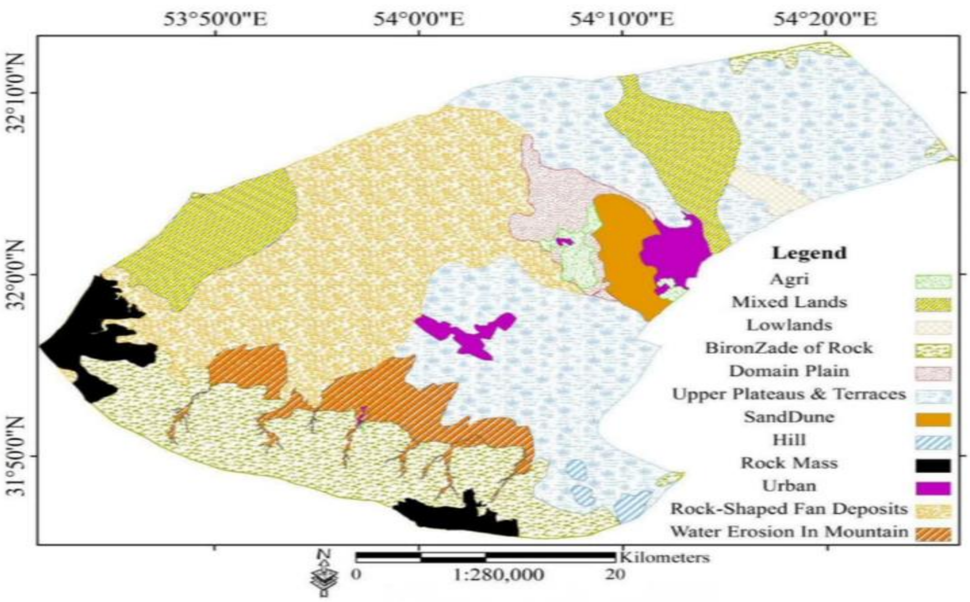

Fig. 4. Works-unit map in Northwest of Yazd (geomorphological Facies)

3.2 Desertification in the basic period

The quantitative value map of desertification of rainfall, dryness and drought persistence index is shown in Figure 5. Considering that the maximum length of the consecutive drought period in all stations of the research area is the same and three years, the amount of drought continuity index in all work units was considered the same and 1.5. Based on Figure 5, the UTI aridity index has the greatest impact on the intensity of desertification in the region. In this index and rainfall index, the flat areas located in the center and east of the region have more desertification intensity than the mountainous areas located in the west and southwest. The highest desertification score in both mentioned indexes is related to sand dunes.

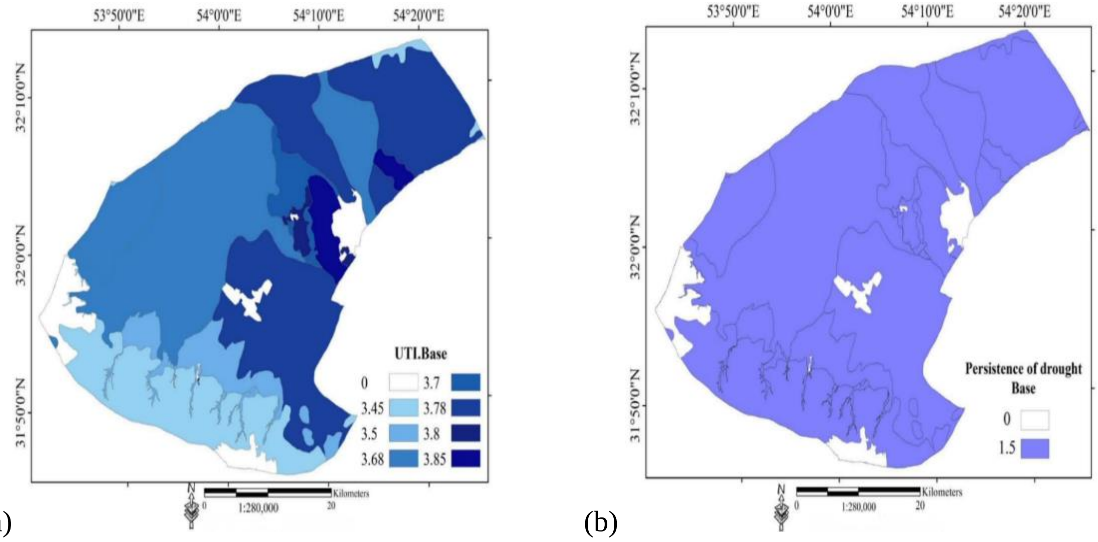

(a) (b)

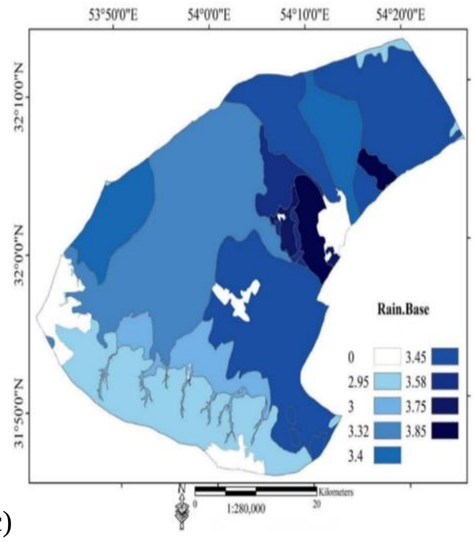

(c)

Fig. 5. Desertification class map: a) precipitation index, b) drought index and c) drought persistence index in the base period.

From the geometric mean of the maps of the mentioned indicators, a map of desertification was prepared based on the climate criteria. Quantitative map and qualitative class of desertification based on climate criteria are presented in Figure 6. The risk class map of the desertification intensity of the region shows that the number of three classes low (4.55%), medium (14.91%) and severe (80.54%) have been identified in the region, and the highest level is the severe class.

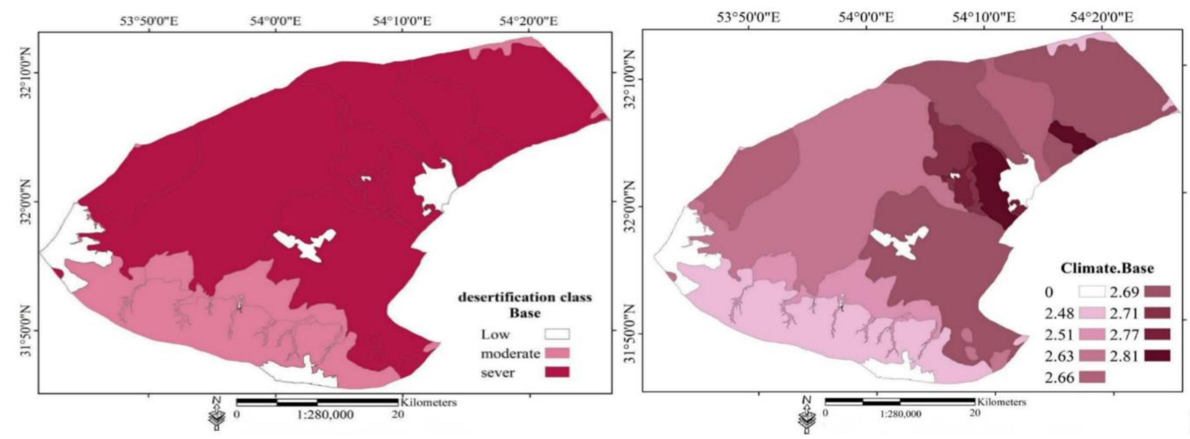

Fig. 6. Quantitative and qualitative map of the desertification risk class in the base period

Finally, based on the weighted average of the indicators evaluated in the desertification of the region, the final score of the intensity of desertification of the entire research area was 2.67. Comparing it with the classification in Table 2, the final class of the intensity of desertification in the region is severe.

IMDPA is the final quantity of the intensity of desertification in the region with the model= 〚 (precipitation of weighted average index × drought of weighted average index × drought of continuity of weighted average index) 〛 ^ $(\frac{1}{3})$

The final quantity of desertification intensity of the region with the IMDPA model in the base period= $= \sqrt[3]{3.46 \times 3.68 \times 1.5} = 2.67$

3.3. Forecasting climate elements in the future based on climate change models

3.3.1. Performance evaluation of LARS-WG6

The performance evaluation of LARS-WG6 in the simulation of monthly parameters of rainfall and average temperature for the base period (2001-2020) in selected stations is presented in Table 5. Based on the results of this table, the high explanatory coefficient (R^2) in all stations and the low values of MAE and NRMSE <20% of climatic elements indicate the high performance and ability of the model in simulating the climatic data of the basin in the statistical period.

Table 5. LARS-WG model evaluation results for rainfall and average monthly temperature of the stations

Station Name	Tmean			Rain		
	R^2	NRMSE%	MAE	R^2	NRMSE%	MAE
Yazd	0.994	0.90	0.19	0.87	16.14	0.83
Ashkezar	0.991	1.37	0.25	0.91	10.79	0.70
KhezrAbad	0.995	0.81	0.15	0.93	10.42	1.45
Meibood	0.993	0.89	0.19	0.95	9.89	0.72
Nodoshan	0.994	0.88	0.18	0.96	9.88	9.88

3.3.2. Change of climatic elements in the near future (period 2026-2055)

As Figure 6 shows, the temperature will increase in all three scenarios at all stations in the near future, and the amount of this increase is higher in RCP8.5 than in other scenarios. The lowest and highest annual temperature increase is related to Ashkezar station (RCP2.6) and Khezrabad station (RCP8.5) by +0.58 and +1.19 (°C). In the period 2026-2055, the monthly rainfall will vary between -5.49 (mm) (Nadoshan, January and RCP4.5) to +5.04 (mm) (Meibood, December and RCP2.6). The biggest decrease and increase in annual rainfall are related to Nodoshan and Yazd stations, respectively, by -5.80 and +10.70 mm. The reason for the increase and decrease of rainfall in these stations can be attributed to the climatic characteristics and the local topography (mountainous or flat). The annual rainfall changes indicate that in the near future, in all three scenarios, rainfall will decrease compared to the base period only at the Nodoshan station. In other stations, rainfall changes in scenario 2.6, which is the most optimistic scenario, increase more than the other two scenarios, and except for Ashkezar station, in other stations, rainfall decreases with the increase of radiative forcing (Fig. 7).

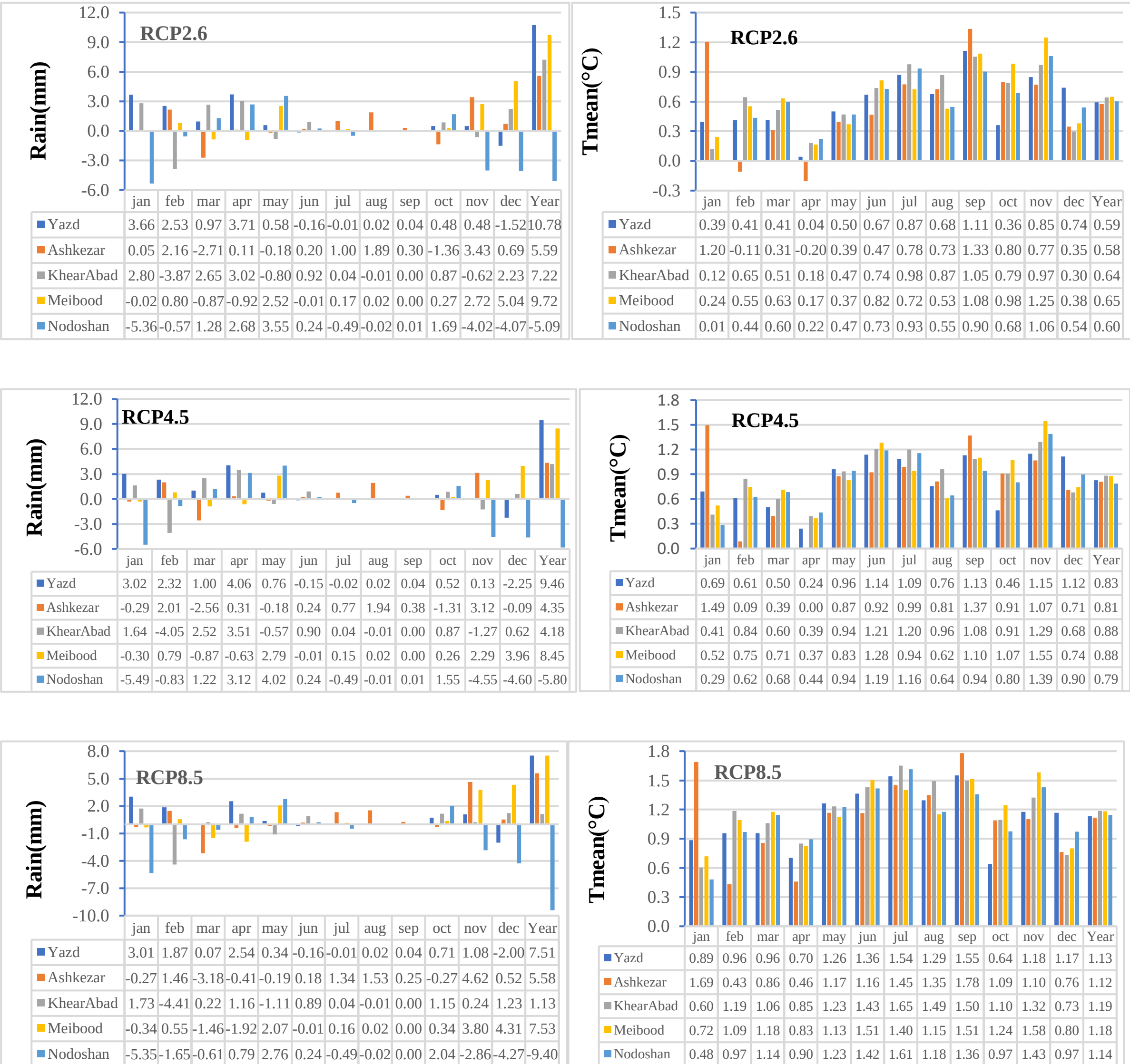

RCP2.6 – Rain(mm)

	jan	feb	mar	apr	may	jun	jul	aug	sep	oct	nov	dec	Year
Yazd	3.66	2.53	0.97	3.71	0.58	-0.16	-0.01	0.02	0.04	0.48	0.48	-1.52	10.78
Ashkezar	0.05	2.16	-2.71	0.11	-0.18	0.20	1.00	1.89	0.30	-1.36	3.43	0.69	5.59
KhearAbad	2.80	-3.87	2.65	3.02	-0.80	0.92	0.04	-0.01	0.00	0.87	-0.62	2.23	7.22
Meibood	-0.02	0.80	-0.87	-0.92	2.52	-0.01	0.17	0.02	0.00	0.27	2.72	5.04	9.72
Nodoshan	-5.36	-0.57	1.28	2.68	3.55	0.24	-0.49	-0.02	0.01	1.69	-4.02	-4.07	-5.09

RCP2.6 – Tmean(°C)

	jan	feb	mar	apr	may	jun	jul	aug	sep	oct	nov	dec	Year
Yazd	0.39	0.41	0.41	0.04	0.50	0.67	0.87	0.68	1.11	0.36	0.85	0.74	0.59
Ashkezar	1.20	-0.11	0.31	-0.20	0.39	0.47	0.78	0.73	1.33	0.80	0.77	0.35	0.58
KhearAbad	0.12	0.65	0.51	0.18	0.47	0.74	0.98	0.87	1.05	0.79	0.97	0.30	0.64
Meibood	0.24	0.55	0.63	0.17	0.37	0.82	0.72	0.53	1.08	0.98	1.25	0.38	0.65
Nodoshan	0.01	0.44	0.60	0.22	0.47	0.73	0.93	0.55	0.90	0.68	1.06	0.54	0.60

RCP4.5 – Rain(mm)

	jan	feb	mar	apr	may	jun	jul	aug	sep	oct	nov	dec	Year
Yazd	3.02	2.32	1.00	4.06	0.76	-0.15	-0.02	0.02	0.04	0.52	0.13	-2.25	9.46
Ashkezar	-0.29	2.01	-2.56	0.31	-0.18	0.24	0.77	1.94	0.38	-1.31	3.12	-0.09	4.35
KhearAbad	1.64	-4.05	2.52	3.51	-0.57	0.90	0.04	-0.01	0.00	0.87	-1.27	0.62	4.18
Meibood	-0.30	0.79	-0.87	-0.63	2.79	-0.01	0.15	0.02	0.00	0.26	2.29	3.96	8.45
Nodoshan	-5.49	-0.83	1.22	3.12	4.02	0.24	-0.49	-0.01	0.01	1.55	-4.55	-4.60	-5.80

RCP4.5 – Tmean(°C)

	jan	feb	mar	apr	may	jun	jul	aug	sep	oct	nov	dec	Year
Yazd	0.69	0.61	0.50	0.24	0.96	1.14	1.09	0.76	1.13	0.46	1.15	1.12	0.83
Ashkezar	1.49	0.09	0.39	0.00	0.87	0.92	0.99	0.81	1.37	0.91	1.07	0.71	0.81
KhearAbad	0.41	0.84	0.60	0.39	0.94	1.21	1.20	0.96	1.08	0.91	1.29	0.68	0.88
Meibood	0.52	0.75	0.71	0.37	0.83	1.28	0.94	0.62	1.10	1.07	1.55	0.74	0.88
Nodoshan	0.29	0.62	0.68	0.44	0.94	1.19	1.16	0.64	0.94	0.80	1.39	0.90	0.79

RCP8.5 – Rain(mm)

	jan	feb	mar	apr	may	jun	jul	aug	sep	oct	nov	dec	Year
Yazd	3.01	1.87	0.07	2.54	0.34	-0.16	-0.01	0.02	0.04	0.71	1.08	-2.00	7.51
Ashkezar	-0.27	1.46	-3.18	-0.41	-0.19	0.18	1.34	1.53	0.25	-0.27	4.62	0.52	5.58
KhearAbad	1.73	-4.41	0.22	1.16	-1.11	0.89	0.04	-0.01	0.00	1.15	0.24	1.23	1.13
Meibood	-0.34	0.55	-1.46	-1.92	2.07	-0.01	0.16	0.02	0.00	0.34	3.80	4.31	7.53
Nodoshan	-5.35	-1.65	-0.61	0.79	2.76	0.24	-0.49	-0.02	0.00	2.04	-2.86	-4.27	-9.40

RCP8.5 – Tmean(°C)

	jan	feb	mar	apr	may	jun	jul	aug	sep	oct	nov	dec	Year
Yazd	0.89	0.96	0.96	0.70	1.26	1.36	1.54	1.29	1.55	0.64	1.18	1.17	1.13
Ashkezar	1.69	0.43	0.86	0.46	1.17	1.16	1.45	1.35	1.78	1.09	1.10	0.76	1.12
KhearAbad	0.60	1.19	1.06	0.85	1.23	1.43	1.65	1.49	1.50	1.10	1.32	0.73	1.19
Meibood	0.72	1.09	1.18	0.83	1.13	1.51	1.40	1.15	1.51	1.24	1.58	0.80	1.18
Nodoshan	0.48	0.97	1.14	0.90	1.23	1.42	1.61	1.18	1.36	0.97	1.43	0.97	1.14

Fig. 7. The changes of the predicted climatic elements of all stations in the near future (2055-2026) compared to the base period in three radiative forcing scenarios (RCP8.5, 4.5, 2.6)

3.3.3. Change of climatic elements in the distant future (period 2071-2100)

According to Figure 8, the average temperature at the end of this century (period 2071-2100) in all scenarios is higher than the average of the base period, and as the radiative forcing scenario increases, the average temperature also increases and the amount of these changes in this period is more than it is the previous course. The highest and lowest temperature changes respectively for Ashkezar in September by RCP8.5 (+5.17°C) and Nodoshan in January was predicted by RCP2.6 (-0.20°C). Annual average temperature changes are fluctuating from +0.79 to +3.81 (°C). The amount of rainfall changes in the far future, except for the Ashkezar station and the optimistic and pessimistic radiative forcing scenarios, in other stations and all scenarios, is less than the near future. Therefore, the rainfall in the far future will decrease in the region compared to the near future, and the rainfall will increase in some places and decrease in others compared to the base period. The highest decrease in monthly rainfall in the period of 2071-2100 is related to Nodoshan station in January and the pessimistic radiative forcing scenario to the amount of -5.41 mm, and the highest increase is related to Meibood station in December and the optimistic radiative forcing scenario. It is +6.59 mm (Fig. 8).

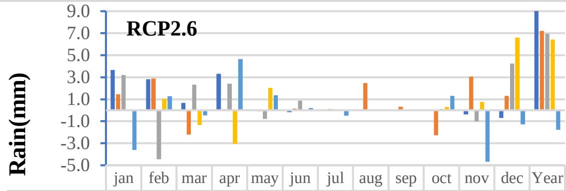

	jan	feb	mar	apr	may	jun	jul	aug	sep	oct	nov	dec	Year
Yazd	3.66	2.83	0.68	3.32	-0.04	-0.18	-0.03	0.02	0.01	-0.06	-0.39	-0.71	9.10
Ashkezar	1.44	2.88	-2.20	0.08	-0.10	0.14	0.10	2.47	0.31	-2.26	3.05	1.31	7.22
KhearAbad	3.21	-4.45	2.33	2.42	-0.78	0.86	0.05	-0.01	0.00	0.11	-1.01	4.24	6.95
Meibood	0.05	1.05	-1.35	-3.06	2.03	-0.01	0.03	0.04	0.00	0.30	0.76	6.59	6.43
Nodoshan	-3.60	1.28	-0.46	4.64	1.36	0.20	-0.49	-0.02	-0.01	1.30	-4.70	-1.29	-1.77

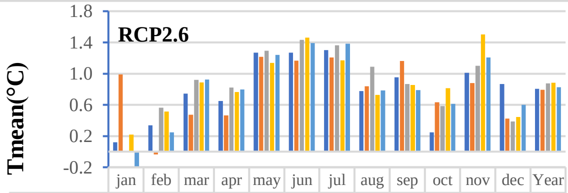

	jan	feb	mar	apr	may	jun	jul	aug	sep	oct	nov	dec	Year
Yazd	0.12	0.34	0.74	0.65	1.27	1.27	1.30	0.78	0.95	0.25	1.01	0.87	0.80
Ashkezar	0.99	-0.04	0.47	0.47	1.22	1.17	1.21	0.84	1.16	0.63	0.88	0.42	0.79
KhearAbad	-0.01	0.56	0.92	0.82	1.29	1.43	1.36	1.09	0.87	0.58	1.10	0.39	0.87
Meibood	0.22	0.52	0.89	0.76	1.14	1.46	1.17	0.73	0.86	0.81	1.50	0.44	0.88
Nodoshan	-0.20	0.25	0.92	0.80	1.24	1.39	1.38	0.78	0.79	0.61	1.21	0.60	0.82

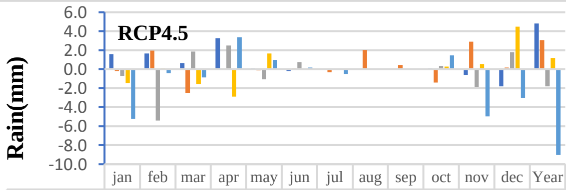

	jan	feb	mar	apr	may	jun	jul	aug	sep	oct	nov	dec	Year
Yazd	1.58	1.66	0.63	3.29	0.12	-0.19	-0.04	0.02	0.03	0.12	-0.59	-1.81	4.82
Ashkezar	-0.19	1.95	-2.51	0.06	-0.12	0.11	-0.33	2.01	0.44	-1.42	2.90	0.16	3.07
KhearAbad	-0.71	-5.40	1.87	2.49	-1.07	0.76	0.03	-0.01	0.00	0.34	-1.88	1.78	-1.80
Meibood	-1.47	0.12	-1.57	-2.87	1.65	-0.01	-0.02	0.03	0.00	0.27	0.56	4.49	1.17
Nodoshan	-5.23	-0.43	-0.87	3.38	1.00	0.17	-0.50	-0.03	0.00	1.45	-4.95	-3.02	-9.05

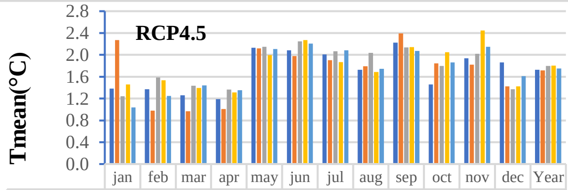

	jan	feb	mar	apr	may	jun	jul	aug	sep	oct	nov	dec	Year
Yazd	1.38	1.37	1.26	1.19	2.13	2.08	2.01	1.73	2.22	1.46	1.94	1.86	1.73
Ashkezar	2.27	0.98	0.97	1.01	2.12	1.98	1.90	1.79	2.39	1.85	1.82	1.42	1.72
KhearAbad	1.24	1.59	1.43	1.37	2.15	2.25	2.07	2.04	2.14	1.80	2.02	1.37	1.79
Meibood	1.46	1.53	1.39	1.31	1.99	2.27	1.87	1.69	2.14	2.05	2.45	1.43	1.80
Nodoshan	1.04	1.25	1.44	1.36	2.11	2.20	2.08	1.74	2.07	1.86	2.15	1.61	1.75

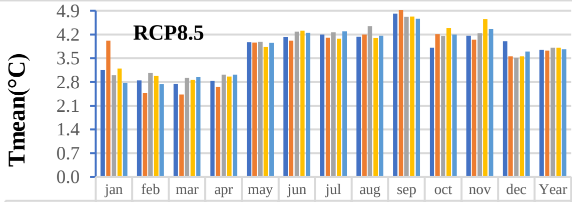

	jan	feb	mar	apr	may	jun	jul	aug	sep	oct	nov	dec	Year
Yazd	3.15	2.85	2.74	2.84	3.97	4.13	4.20	4.13	4.81	3.81	4.16	4.00	3.74
Ashkezar	4.02	2.47	2.43	2.66	3.96	4.02	4.10	4.20	4.95	4.21	4.04	3.55	3.73
KhearAbad	3.00	3.06	2.92	3.02	3.99	4.29	4.27	4.45	4.72	4.15	4.24	3.50	3.81
Meibood	3.20	2.98	2.87	2.96	3.83	4.32	4.07	4.10	4.73	4.39	4.66	3.55	3.81
Nodoshan	2.77	2.73	2.94	3.02	3.95	4.25	4.29	4.16	4.66	4.20	4.36	3.69	3.76

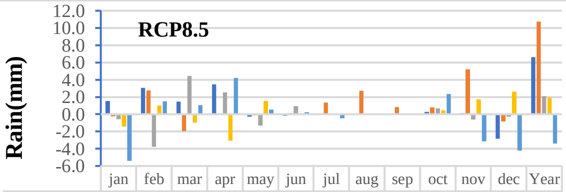

	jan	feb	mar	apr	may	jun	jul	aug	sep	oct	nov	dec	Year
Yazd	1.53	3.05	1.46	3.46	-0.29	-0.16	-0.02	0.02	0.01	0.27	0.12	-2.84	6.60
Ashkezar	-0.26	2.75	-1.94	0.09	-0.13	0.13	1.36	2.74	0.84	0.79	5.22	-0.85	10.73
KhearAbad	-0.57	-3.78	4.42	2.56	-1.31	0.95	0.07	-0.01	0.00	0.68	-0.63	-0.29	2.09
Meibood	-1.42	1.00	-0.99	-3.06	1.52	-0.01	0.10	0.04	0.00	0.44	1.73	2.61	1.96
Nodoshan	-5.41	1.50	1.04	4.20	0.52	0.23	-0.48	-0.01	0.02	2.34	-3.15	-4.20	-3.41

Fig. 8. Changes of predicted climate elements of all stations in the far future (2071-2100) compared to the base period in three radiative forcing scenarios (RCP8.5, 4.5, 2.6)

3.4. Evaluation of desertification in the near and distant future

The score map of the indicators of precipitation amount, dryness index and drought duration in the evaluation of climate criteria in desertification of the research area in all three scenarios RCP2.6, RCP4.5 and RCP8.5 for the near and far future are presented in figures 9 to 11. The intensity of desertification of the precipitation index in the near future and RCP8.5 is a little more intense than the base period. The UTI aridity index score in all three scenarios in the far future is higher than the near future and the base period, so that the desertification intensity score has reached 4 in the pessimistic scenario (RCP8.5). The index score of drought persistence in the near future is similar to the base period, and in the far future it is higher than the base period.

Figure 12 shows the severity of IMDPA desertification based on climate criteria for the near future and the far future with the BCC-CSM1-1 model under three scenarios. As can be seen, the desertification intensity of the climate criterion in the far future is more intense than the near future and the base period (Figure 6). The maximum desertification intensity of the climate criterion in the base period is related to the sand dunes work unit with a score of 2.81, and the maximum score of this unit in the distant future in the moderate radiative forcing scenario (RCP4.5) is arrive 3.13.

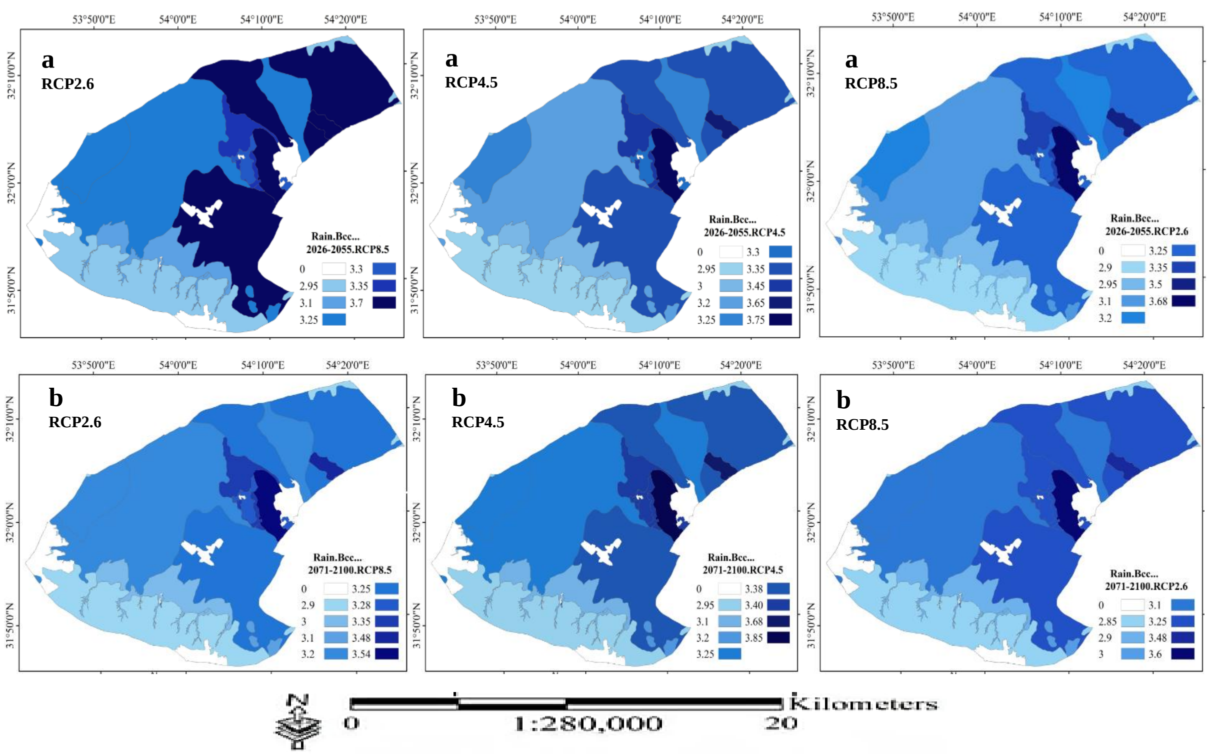

Fig. 9. Desertification intensity of rainfall index for the period 2055-2026 (near future, a) and 2100-2071 period (far future, b) in RCP2.6, 4.5, 8.5 scenarios

The map of the desertification risk class as an example only in the RCP8.5 scenario in the near and far future is presented in Figure 13, and the comparison of the desertification risk classes of all scenarios in both periods is presented in Figure 13. According to Figure 12, in the near future, the region will be in three classes of low, moderate, and severe desertification, but in the near future, the region will be in low, severe, and very severe classes. The comparison of the desertification risk class of the region (Figure 14) shows that in the near future, in RCP2.6

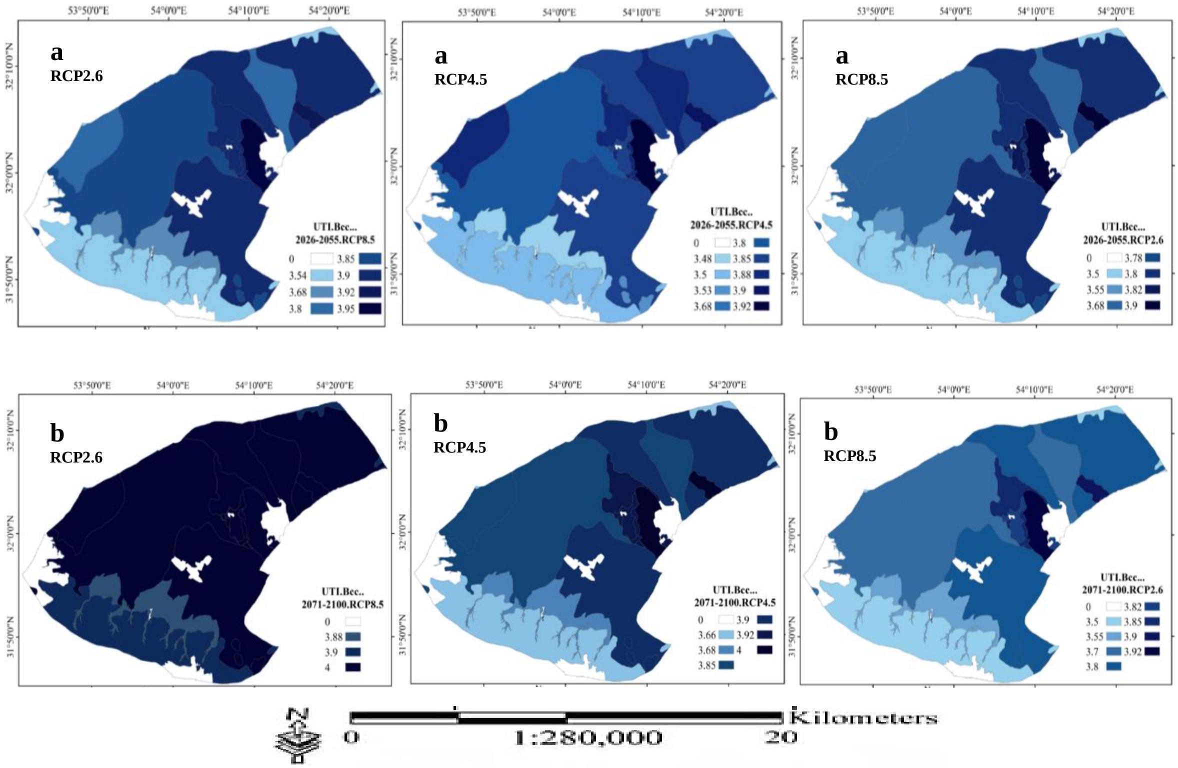

Fig. 10. Intensity of desertification of drought index for the period 2055-2026 (near future, a) and 2100-2071 period (far future, b) in RCP2.6, 4.5, 8.5 scenarios

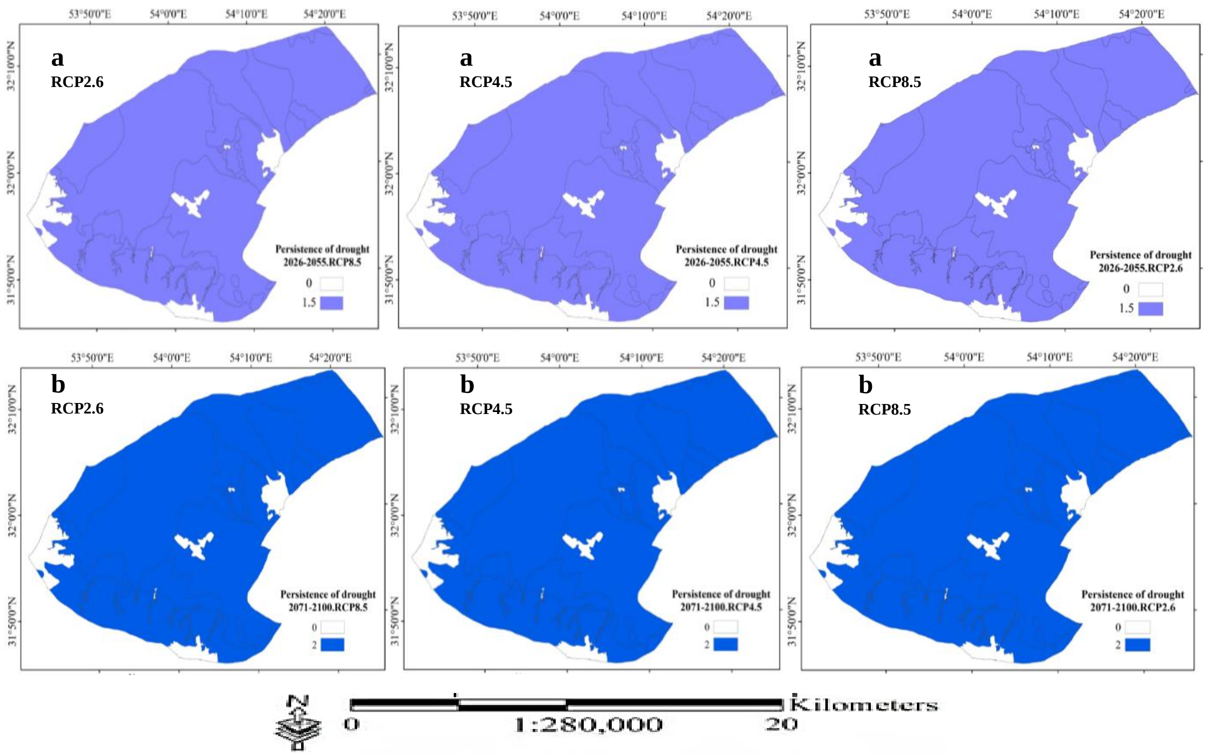

Fig. 11. Intensity of desertification, index of drought continuity for the period 2055-2026 (near future, a) and 2100-2071 period (far future, b) in RCP2.6, 4.5, 8.5 scenarios

and RCP4.5, there will be slight changes in the moderate and severe class, which will increase and decrease, respectively. So that the average class area percentage in both scenarios increases from 14.91% to 20.78% and the extreme class area percentage decreases from 80.54% to 74.67%. In the near future and RCP8.5, there will be no change compared to the base period. In the distant future, the percentage of the area of the average class will decrease and the extreme and very intense classes will increase; This increase in extreme class will be from 36.92% in RCP4.5 and RCP8.5 to 14.93% in RCP2.6. In the very extreme class, this increase is predicted from 2.31% in RCP2.6 to 3.09% in RCP4.5 and RCP8.5.

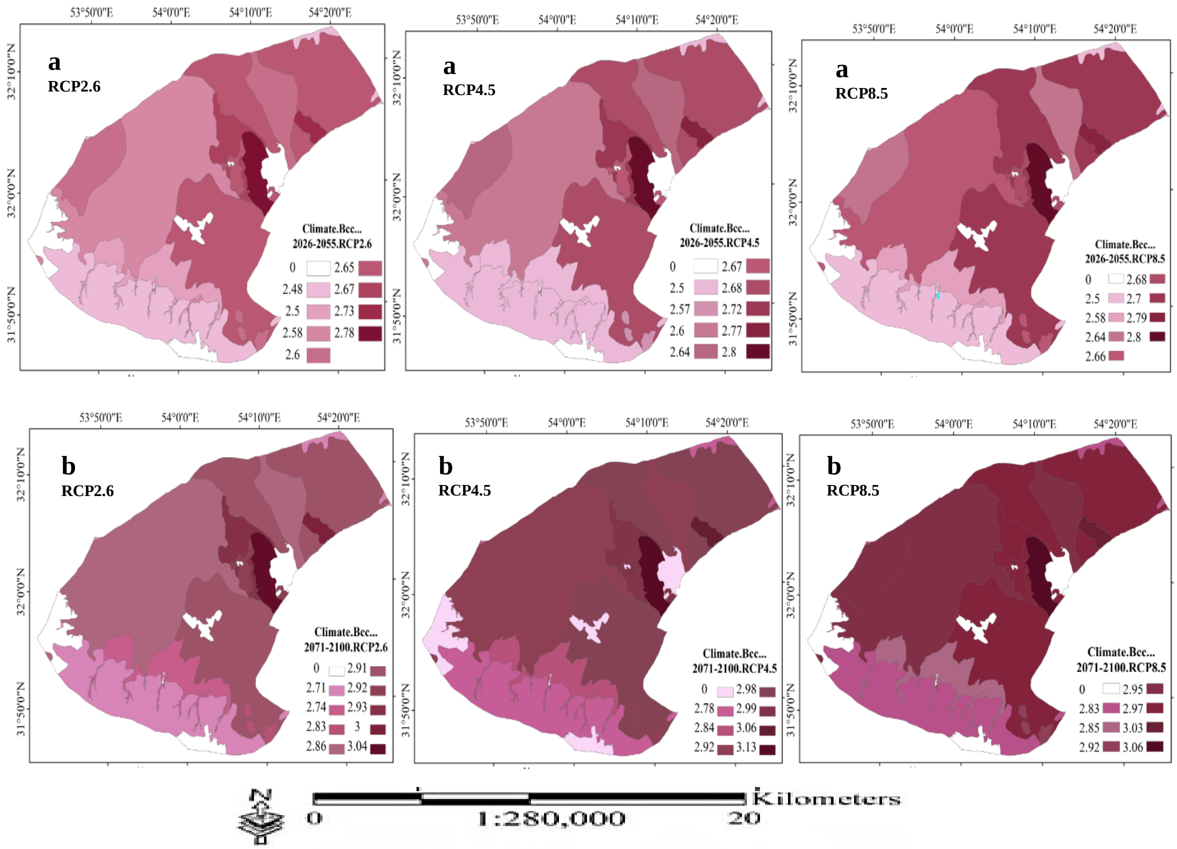

Fig. 12. Intensity of climate standard desertification for the period 2055-2026 (near future, a) and 2100-2071 (far future, b) in RCP2.6, 4.5, 8.5 scenarios

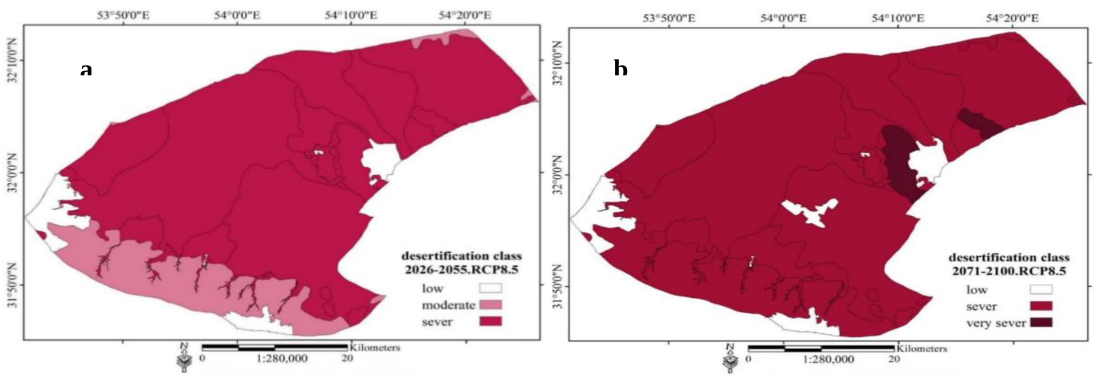

Fig. 13. Qualitative class map of desertification in the near future (a) and far future (b) based on RCP8.5

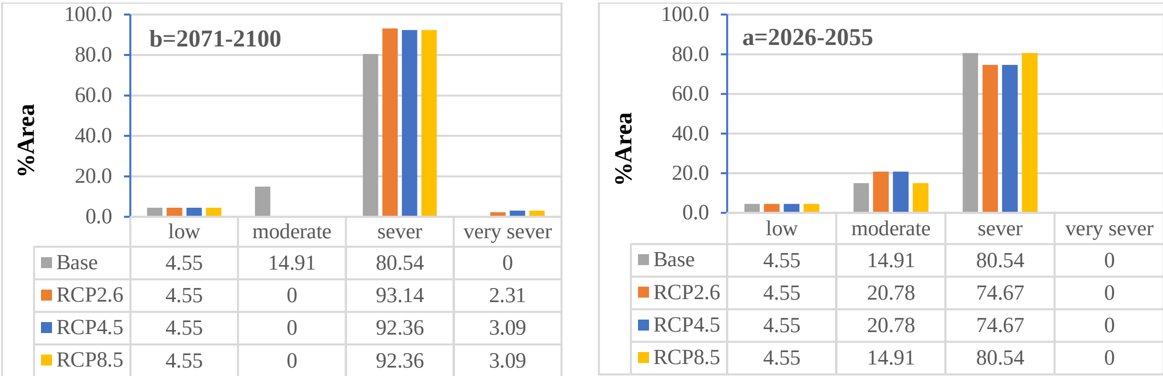

Fig. 14. Comparison of desertification risk classes of scenarios in the near future (a) and far future (b)

The final score of the desertification intensity of the entire research area in the future is calculated based on the weighted average of the climatic indicators evaluated in the desertification of the area in the future periods based on the BCC-CSM1-1 model and presented in Table 6. Based on the results of this table, the final intensity of desertification of the entire research area has decreased slightly compared to the base period in the near future and increased in the distant future. As mentioned earlier, the temperature in the region will increase in the future. Rainfall is also increasing, and this increase in rainfall will be more likely in the form of floods and showers. With the increase of rainfall, the effect of rainfall index and drought persistence index on the desertification of the region in the future periods will decrease compared to the base period. Only the aridity index that is affected by rainfall and temperature has the greatest impact on the intensity of desertification in the research area in the future. Finally, with the geometric averaging of climate indicators in the assessment of climate criteria, the intensity of desertification in the region will not change much in the future periods, and the research area in all three radiative forcing scenarios in the future periods will be in the extreme class. Desertification is placed.

Table 6- The final quantity of desertification intensity of the entire research area in the future

Baseline	Near Feature (2026-2055)			Fae feature (2071-2100)		
	RCP2.6	RCP4.5	RCP8.5	RCP2.6	RCP4.5	RCP8.5
2.67	2.62	2.64	2.67	2.88	2.96	2.95

4. Discussion and Conclusion

In this research, the IMDPA model was used to evaluate desertification in the northwest of Yazd. Also, the annual values of rainfall and average temperature data in the near future and the far future were evaluated with the GCM-CMIP5 model with three forecast radiative forcing scenarios and how their occurrence affects the intensity of desertification in the future.

The results of the evaluation of the error statistics related to the simulation of the BCC-CSM1-1 model used in LARS-WG6 showed that this model has the lowest amount of error statistics, especially the acceptable NRMSE, and the values are closer to the temperature and rainfall data. Meteorological stations determine the region and the results of this model can be trusted in predicting climate elements in the near future and the far future. From examining the output of the graphs in the future, it is clear that the forecasted average temperature changes compared to the base period have a regular and increasing rhythm, and the results are consistent with the results of (Almazroui *et al*., 2017; Javaherian *et al*., 2021). In all stations, the average temperature at the end of this century (period 2071-2100) in all scenarios is higher than the average of the base period and the near future, and as the radiative forcing scenario increases, the average temperature also increases. The annual average temperature changes in the distant future from the 2.6 to 8.5 scenario are fluctuating from +0.79 to +3.81 (℃), respectively. The rhythm of monthly and annual rainfall changes from 2026-2055 to 2071-2100 will fluctuate for different models and scenarios. Also, based on the outputs from the set of GCM-RCP scenarios in predicting the rainfall parameter in the future, it was concluded that the rainfall of the research stations in the last decades of this century, from the period of 2026-2055, is lower and in some places compared to the average of the base period, increasing or it is a reduction. Therefore, based on the climatic features and the local topography, the only area that will face an increase in rainfall at the end of this century is the flat and central region of Yazd, although the increase in rainfall in this area is unaffected by the relative increase in temperature, while the rainfall behavior of this region in the future will be in the form of sudden and torrential rains. The mountainous areas located in the west and south-west will also face a decrease in rainfall in the future. The increase of rainfall in the future is consistent with the research results of (Mahmood and Babel, 2013) and the decrease of rainfall is also consistent with the research results of (Almazroui *et al*., 2017). Finally, the climatic conditions of the research area in the future periods will be significantly different from the conditions of the base period.

The quantitative and qualitative map of the intensity of desertification of the research area using the IMDPA model showed that the largest area of the research area with an area of 80.54% is in the extreme class of desertification, which is in accordance with the results of (Lee *et al*., 2019). Finally, the entire research area was placed in the severe class with a final desertification intensity score of 2.76. Among the investigated climatic indicators, the dryness index, being in the very severe class (score 3.68), has had the greatest effect on the desertification of the region. Then there is the index of rainfall (3.46) and the persistence of drought (1.5).

The climate parameters obtained for all three scenarios in the future periods were re-entered into the IMDPA model in order to evaluate the impact of climate change on the indicators effective in desertification. The results of forecasting climate indicators in the evaluation of desertification in the research area clearly show that the intensity of desertification of rainfall index in the near future and RCP8.5 is a little more intense than the base period. The score of drought persistence index in all scenarios is higher in the distant future than in the near future. The Drought Index score (UTI) in all scenarios at the end of this century is higher than the near future and base period, so that in the pessimistic scenario (RCP8.5), the desertification intensity score has increased to 4, which indicates an increase in the intensity of drought. It is in the research area. Also, the score of desertification caused by the climate criterion is higher in the distant future than in the near future, and this score is higher in the sand dunes and lowland work units than in other work units. Therefore, the prediction of the desertification model in different climate scenarios provides different results.

As shown in Table 6, the final desertification intensity of the entire research area has slightly decreased in the near future compared to the base period and has slightly increased in the distant future. The largest increase is associated with RCP4.5. In the future, as temperatures increase in the research area, precipitation will also increase. And this increase in precipitation will be offset by the relative increase in temperature. And the average temperature parameter will have the most influential fluctuation in the future climate. Therefore, among the climatic indicators, only the drought index, which is affected by rainfall and temperature, will have the greatest impact on the intensity of desertification in the research area in the future. Finally, by considering the geometric mean of climate indicators in assessing climate criteria, the desertification risk class of the region will not change in future periods. And the research area will be in the severe desertification class in all three radiative forcing scenarios in the future periods. Therefore, due to the reasons mentioned, climate change models will be able to predict the extent and changes of desertification in the future.

According to the results of the increase in temperature, the lack of simulated rainfall in summer and the decrease in rainfall in the last decades of this century, an improvement of knowledge was obtained in relation to the situation in the northwest region of Yazd. There will be possible consequences of this situation in the future, such as increased evaporation and transpiration, increased plant water requirements, decreased seed germination and vegetation cover, decreased soil microbial flora, decreased soil quality, decreased soil water and groundwater recharge, increased wind speed., the increase of wind erosion and the creation of dust storms are accompanied, And in general, these changes, along with a lot of human impact, such as excessive livestock grazing, overexploitation of underground water, conversion of pastures into agricultural lands and facilities, destruction of vegetation and bush cutting, cause the destruction of pastures and natural resources, and as a result, the significant reduction of areas Humid climate and the increase in dry climate and severe drought, and these are the reasons that cause the increase in the level of the desert and the spread of the phenomenon of desertification in the research area, which may result in the destruction of the ecosystem, the threat of vital systems and settlements, and finally the effects It has adverse effects on human life and health.

It is suggested to provide this field by reducing the effective technologies in the increase of carbon dioxide and adding biological appendages to industrial development plans and using more renewable energy. Also, due to the fact that climatic changes and irregularities are becoming common and the results of forecasting climatic elements in this research also show the same, it is suggested that rainwater harvesting systems be taken into consideration and it should be used in planning for managing water resources and expanding vegetation in the region. Vegetation and ecosystem management should be done by examining the function of up-to-date models and indicators in evaluating the intensity of desertification with emphasis on early warning systems and protecting and controlling the exploitation of vegetation in order to strengthen the natural cover of ecosystems.

Author Contributions

For research articles with several authors, a short paragraph specifying their individual contributions must be provided. The following statements should be used "Conceptualization, Azam Sadat Hosseini Khezrabad[1]. and Abbas Ali Vali[2].; methodology, Azam Sadat Hosseini Khezrabad[1].; software, Amirhossein Halabian[3].; validation, Abbas Ali Vali[2], Amirhossein Halabian[3]. and Azam Sadat Hosseini Khezrabad[1].; formal analysis, Abbas Ali Vali[2].; investigation, Mohammad Hossein Mokhtari[4].; resources, Mohammad Hossein Mokhtari[4].; data curation, Seyed Ali Mousavi[5].; writing—original draft preparation, Seyed Ali Mousavi[5].; writing—review and editing, Seyed Ali Mousavi[5].; visualization, Seyed Ali Mousavi[5].; supervision, Abbas Ali Vali[2].; project administration, Abbas Ali Vali[2].; funding acquisition, Seyed Ali Mousavi[5]. All authors have read and agreed to the published version of the manuscript.

Data Availability Statement

"Not applicable"

Acknowledgements

The authors of this study express their gratitude to Kashan University and the respected professors for their material and moral support.

Acknowledgements

The authors of this study express their gratitude to University of Kashan and the respected professors for their material and moral support.

Ethical considerations

The authors avoided from data fabrication and falsification.

Funding

The study was funded by the University of Kashan, Country Iran, and without Grant for Dr Abbasali Vali Associated Professor at University of Kashan. This research did not receive any specific grant from funding agencies in the public, commercial, or not-for-profit sectors.

Conflict of interest

"The funders had no role in the design of the study; in the collection, analyses, or interpretation of data; in the writing of the manuscript, or in the decision to publish the results".

References

Abbasian, M. S., Moghim, S., & Abrishamichi, A. (2018). Performance of the general circulation models in simulating temperature and precipitation over Iran. *Theoretical and Applied Climatology*, 135(3-4), 1465- 1483. https://doi:10.1007/s00704-018-2456y

Abuzaid, A. S., & Abdelatif, A. D. (2022). Assessment of desertification using modified MEDALUS model in the north Nile Delta, Egypt. *Geoderma*, 45, 115400. https://doi.org/10.1016/j.geoderma.2021.115400

Ahmadi, H. (2006). Calibration of measurement and standards of desertification in Iran, IMDPA model, Client: Department of Pasture and Soil of Forest, Rangeland and Watershed Management.

Akbari, M., Ownegh, M., Asgari, H. R., Sadoddin, A., Khosravi. H. (2016). Desertification risk assessment and management program. *Global Journal Environmental Science Management*, 2(4), 365-380. https://doi.org/10.22034/gjesm.2016.02.04.006

Almazroui, M., Nazrul Islam, M., Saeed, F., Alkhalaf, A. K., & Dambul, R. (2017). Assessing the robustness and uncertainties of projected changes in Temperature and Precipation in AR5 Global Climate Models Over the Arabian Peninsula. *Atmospheric research*, 194, 202-213. https://doi.org/10.1016/j.atmosres.2017.05.005

Alori, E.T., Emmanuel, O. C., Glick, B. R., & Babalola, O. O. (2020). Plant–archaea relationships: a potential means to improve crop production in arid and semi-arid regions. *World Journal of Microbiology and Biotechnology*, 36, 1–10. https://doi.org/10.1007/s11274-020-02910-6

Arami, A. H., Ownegh, M., Sheikh, B., & Honardoust, F. (2012). Desertification assessment and mapping desertification severity using IMDPA with emphasis on vegetation and soil criteria in the GIS environment (Case study: Alagol Plain, Golestan Province. First national desert Conference. Tehran, International Research Center for desert. Tehran University, Iran. https://civilica.com/doc/160382

Arami. S. A., & Ownagh, M. (2017). Assessment of desertification hazard, risk and development of management plans. *Desert*, 22(1), 51-67. https://sid.ir/paper/716366/en

Gulacha, M., & Mulungu, D. M. M. (2017). Generation of climate change scenarios for precipitation and temperature at local scales using SDSM in Wami-Ruvu River Basin Tanzania. *Physics and Chemistry of the Earth*, 100, 62-72. https://doi.org/10.1016/j.pce.2016.10.003

Intergovernmental Panel on Climate Change (IPCC). (2014). AR5 Climate Change 2014: Mitigation of Climate Change. Working group III contribution to the IPCC Fifth Assessment Report. 1-49.

Javaherian M. R., Ebrahimi, H., & Aminnejad, B. (2021). Prediction of changes in climatic parameters using CanESM2 model based on RCP scenarios (case study: Lar dam basin). *Ain Shams Engineering Journal*, 1, 445-454. https://doi.org/10.1016/j.asej.2020.04.012

Lee, E. J., Piao, D., Song, C., Kim, J., Lim, H., Kim, E., Moon, J., Kafatos, M., Lamchin, M., Jeon, S. W., & Lee, W. (2019). Assessing environmentally sensitive land to desertification using MEDALUS method in Mongolia. *Forest Science and Technology*, 15(4), 210-220. https://doi.org/10.1080/21580103.2019.1667880

Leon-Sobrino, C., Ramond, J. B., Maggs-Kolling, G., & Cowan, D. A. (2019). Nutrient acquisition, rather than stress response over diel cycles, drives microbial transcription in a hyper-arid Namib Desert soil. *Frontiers in Microbiology*, 10, 1054. https://doi.org/10.3389/fmicb.2019.01054

Mahmood. R., & Babel, M. S. (2013). Evaluation of SDSM developed by annual and monthly sub-models for downscaling temperature and precipitation in the Jhelum basin, Pakistan and India. *Theoretical and Applied Climatology*, 113, 27-44. https://doi.org/10.1007/s00704-012-0765-0

Pellegrini. S., Agnelli, A. E., Andrenelli, M. C., Barbetti, R., Lo Papa, G., Priori, S., & Costantini, E. A. C. (2018). Using present and past climosequences to estimate soil organic carbon and related physical quality indicators under future climatic conditions. *Agriculture, Ecosystems and Environment*, 266, 17–30. https://doi.org/10.1016/j.agee.2018.07.015

Perez-Marin, A. M., Cavalcante, A. M. B., De Medeiros, S. S., Tinoco, L., Salcedo, I. H. (2012). Nucleos de desertificacao no semiarido brasileiro: Ocorrencia natural ou antropica? Parcer. Estrategica. *ReaserchGate*, 17, 87–106. https://bibliotecasemiaridos.ufv.br/jspui/handle/123456789/2561

Perez-Marin, A. M., Vendruscolo, J., Zárate-Salazar, J. R., De Araújo Queiroz, H. A., Magalhães, D. L., Menezes, R. S. C., & Médice Fernandes, R. (2022). Monitoring Desertification Using a Small Set of Biophysical Indicators in the Brazilian Semiarid Region. *Soil Conservation and Sustainability*, 14(15), 9735. https://doi.org/10.3390/su14159735

Pinheiro Junior, C. R., Pereira, M. G., Oseas de Filho, J., & Beutler, S. J. (2019). Can topography affect the restoration of soil properties after deforestation in a semiarid ecosystem? *Journal of Arid Environments*, 162, 45–52. https://doi.org/10.1016/j.jaridenv.2018.11.004

Purkey, D .R., Joyce, B., Vicuna, S., Hanemann, M. W., Dle, L. l., Yates, D., & Dracup. J. A. (2008). Robust Analysis of Future Climate Change Impacts on Water for Agriculture and Other Sectors: A Case Study in the Sacramento Valley. *Climatic Change*, 87, 109–122. DOI 10.1007/s10584-007-9375-8

Refsgaard, J.C., Arnbjerg-Nielsen, K., Drews, M., Halsnaes, K., Jeppesen, E., Madsen, H., Markandya, A., Olesen, J. E., Porter, J. R., & Christensen, J. H. (2013). The role of uncertainty in climate change adaptation strategies– A Danish water management example. *Mitigation and Adaptation Strategies for Global Change*, 18, 337-359. https://doi.org/10.1007/s11027-012-9366-6

Sadeghiravesh, M. H., Khosravi, H., Abolhasani, A., Ghodsi, M., & Mosavi, A. (2021). Fuzzy logic model to assess desertification intensity based on vulnerability indices. *Acta Polytechnica Hungarica*, 18(3), 6-24. https://acta.uni-obuda.hu/Sadeghiravesh_Khosravi_Abolhasani_Ghodsi_Mosavi_110.pdf

Semenov, M. A., & Barrow, E. M. (1997). Use of a stochastic weather generator in the development of climate change scenarios. *Climatic Change*, 35, 397–414.

Sepehr, A., Hassanli, A. M., Ekhtesasi, M. R., & Jamali, J. B. (2007). Quantitative assessment of desertifcation in south of Iran using MEDALUS method. *Environmental Monitoring and Assessment*, 134(3), 243-254. DOI 10.1007/s10661-007-9613-6

Sharafati, A., Pezeshki, E., Shahid, S., & Motta, D. (2020). Quantifcation and uncertainty of the impact of climate change on river discharge and sediment yield in the Dehbar river basin in Iran. *Journal of Soils and Sediments*, 20, 2977–2996. https://doi.org/10.1007/s11368-020-02632-0

Shrestha, A., Babel, M. S., Weesakul, S., & Vojinovic, Z. (2017). Developing Intensity Duration Frequency (IDF) Curves under Climate Change Uncertainty: The Case of Bangkok, Thailand. *Journal of Water*, 145, 1-22. https://doi.org/10.3390/w9020145

Tanarhte, M., Hadjinicolaou, P., & Lelieveld, J. (2012). Intercomparison of temperature and precipitation data sets based on observations in the Mediterranean and the Middle East. *Journal of Geophysical Research: Atmospheres*, 117(D12), 1- 24. https://doi.org/10.1029/2011JD017293

UNCCD (United Nations Convention to Combat Desertification). (1994). Convention to Combat Desertification in Countries Experiencing Serious Drought and/or Desertification, particularly in Africa; ONU: Paris, France, 56p.

Zhang, C., Xunming, W., Jinchang, L., & Ting, H. (2020). Identifying the effect of climate change on desertification in northern China via trend analysis of potential evapotranspiration and precipitation. *Ecological Indicators*, 112, 106-141. https://doi.org/10.1016/j.ecolind.2020.106141.